Cell Tissue Res (2008) 334:67–79
DOI 10.1007/s00441-008-0665-x

REGULAR ARTICLE

The rocker bone: a new kind of mineralised tissue?

E. Parmentier · P. Compère · M. Casadevall · N. Fontenelle · R. Cloots · C. Henrist

Received: 23 April 2008 / Accepted: 11 June 2008 / Published online: 30 July 2008

Abstract In some Ophidiiform fishes, the anterior part of the swimbladder is thickened into a hard structure called the "rocker bone", which is thought to play a role in sound production. Although this structure has been described as cartilage or bone, its nature is still unknown. We have made a thorough analysis of the rocker bone in *Ophidion barbatum* and compared it with both classical bone and cartilage. The rocker bone appears to be a new example of mineralisation. It consists of (1) a ground substance mainly composed of proteoglycans (mucopolysaccharide acid) and fibres and (2) a matrix containing small mineralised spherules composed of a bioapatite and fibrils. These spherules are embedded in mineralised cement of a similar composition to the spherules themselves. The rocker bone grows via the apposition of new apatite spherules at its periphery. These spherules are first secreted by the innermost fibroblast layer of the capsule contained in the rocker bone and then grow extracellularly. Blood vessels, which represent the only means of transport for matrix and mineral material, are numerous. They enter the rocker bone via the hyle and ramify towards the capsule. We propose to call this new kind of mineralised tissue constituting the rocker bone "frigolite" (the Belgian name for styrofoam) in reference to the presence of spherules of different sizes and the peculiarity of the rocker bone in presenting a smooth surface when fractured.

Keywords Hydroxyapatite · Rocker bone · Biomineralisation · Swimbladder · Spherule · *Ophidion barbatum* (Teleostei Ophidiidae)

E.P. is a Research Associate of the Belgian National Fund for Scientific Research (FRS-FNRS). This study was supported by grant no. 2.4574.01 from the Fonds National de la Recherche Scientifique, Belgium.

E. Parmentier (✉) · N. Fontenelle
Laboratoire de Morphologie Fonctionnelle et Evolutive,
Institut de Chimie, Bât. B6, Université de Liège,
B-4000 Liège, Belgium
e-mail: E.Parmentier@ulg.ac.be

P. Compère
Laboratoire de Morphologie Ultrastructurale, Institut de Chimie,
Bât. B6, Université de Liège,
B-4000 Liège, Belgium

M. Casadevall
Unitat de Biologia Animal, Department Facultat de Ciències,
Universitat de Girona,
Campus de Montilivi,
17071 Girona, Spain

R. Cloots · C. Henrist
CATμ and Chimie Inorganique Structurale, Institut de Chimie,
Bât. B6c, Université de Liège,
B-4000 Liège, Belgium

Introduction

Bone and cartilage have a mesenchymatous origin and together form the skeleton in teleosts. As with all other forms of connective tissue, bone and cartilage consist of specialised cells and a matrix. Bones are typically made up of three components (Meunier and François 1992; Meunier and Huysseune 1992): (1) bone cells (osteoblasts, osteocytes and osteoclasts); (2) extracellular organic material mainly consisting of collagen fibrils (type I); (3) a mineralised ground substance of proteoglycans and hydroxyapatite crystals, making the bone rigid and strong but brittle. Three kinds of bone tissue can be distinguished on the basis of the three-dimensional organisation of the fibrils: woven-fibred bone, parallel-fibred bone (=pseudolamellar bone) and lamellar bone (Meunier 1989; Meunier

and François 1992). However, osteichthyans can lack trapped cells and/or mineral material, illustrating the expression of the great adaptive trends of bone in the various osteichthyan lineages (Meunier and Huysseune 1992). More than half of all teleost species have acellular bone, which has similar histological features to those of cellular bone, except that osteocytes are missing because the cells are not incorporated into the osseous matrix (Moss 1961, 1963). Moreover, bone is vascularised and is submitted to the processes of resorption and reconstruction (Meunier and Huysseune 1992).

Cartilage presents isogenous groups of chondrocytes located in lacunae and surrounded by an extensive intercellular matrix, rich in proteoglycans. In cartilage, the collagen fibres (type II) are less abundant than in bone and are frequently associated with elastin fibrils (Meunier and François 1992). The eight identified types of cartilage have been categorised into two groups: cell-rich cartilage and matrix-rich cartilage (Benjamin 1990). Although this happens less frequently than with bone, cartilage can become mineralised. Calcospherites appear in the cartilage matrix, in which crystals are radially oriented. Mineralisation extends by fusion of the calcospherites or by progression of the mineralisation front (Huysseune and Sire 1992).

Another type of skeletal tissue is represented by chondroid bone in which chondrocyte-like cells are embedded in a mineralised bone-like matrix, giving the tissue an appearance intermediate between cartilage and bone (Huysseune and Sire 1990; Meunier and Huysseune 1992). Chondroid bone forms when dispersed chondrocyte-like cells, instead of retracting (as during the formation of acellular bone), become trapped in the bone-like matrix that they deposit (Huysseune 1986). This particular type of tissue is mainly found in articular areas and in sites subjected to mechanical stress (Meunier and Huysseune 1992).

The sonic mechanism recently described in *Ophidion barbatum* includes three pairs of sonic muscles, highly transformed vertebrae, a neural arch that pivots and a swimbladder whose anterior end presents a so-called "rocker bone" (Parmentier et al. 2006). The sonic muscles cause the rocker bone to swivel, compressing the swimbladder. The rocker bone might be the result of the transformation of the anterior part of the swimbladder in response to the mechanical stress of the traction transmitted by the different ligaments and muscles inserted into it (Parmentier et al. 2003a, 2003b) and the subsequent sclerification or ossification of the anterior part of the tunica externa of the swimbladder (Howes 1992; Parmentier et al. 2003b). The nature of the rocker bone is, however, still unknown. Rose (1961) noted: "it would appear to be bone except that it lacks the hardness and permanence of bone […] it is possibly cartilage impregnated with calcium salts".

On the basis of histological cross sections (Fig. 1), the rocker bone seems to be neither bone nor cartilage. The aim of this study has been to describe the nature of the rocker bone in *O. barbatum* by using comparisons with its existing mineralised tissues and mineral analyses.

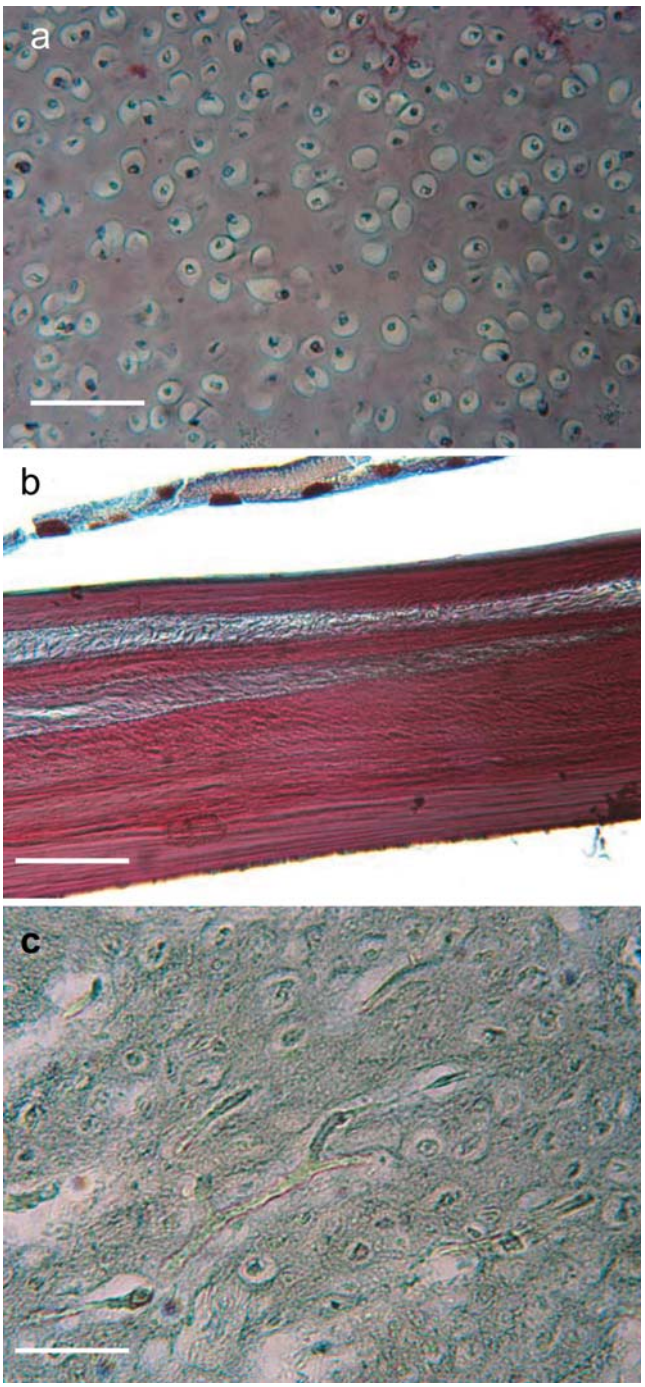

Fig. 1 Histological section of (**a**) cartilage, (**b**) bone and (**c**) rocker bone in *Ophidion barbatum*. Tanzer's colouration. All the tissues were observed on the same section in order to avoid differences caused by the preparation of the material. *Bar* 50 μm

Materials and methods

Biological material

Fifty two specimens of *O. barbatum* (total length: 126–242 mm, width: 173±22 mm) were caught on the Costa Brava (Spain, 41°40′30″ N, 2°47′53″ E) on sandy ground at a depth varying from 90 to 120 m during October 1987, September 2004 and May 2005. Forty-eight fishes were fixed in 7% formaldehyde or in 100% ethanol for dissection and observation of the rocker bone by scanning electronic microscopy (SEM). Two specimens were fixed in Bouin's fluid for serial sectioning.

Rocker bones were taken from the two remaining specimens and were fixed in 2.5% glutaraldehyde for observation by transmission electronic microscopy (TEM). The dentary bones (anterior parts of the mandible) of *O. barbatum* were used to carry out the various comparisons.

The general morphology of the sonic apparatus was examined with a Wild M10 (Leica) stereoscopic microscope equipped with a camera lucida and a digital camera (Canon Power Shot S50). The position of the rocker bone and the skeleton of three specimens were also observed in X-ray photographs (Siemens Tridoros Optimatic 880 X-ray apparatus).

Light microscopy

Bouin-fixed specimens were decalcified for 3 days in a 3% formol-nitric solution before neutralisation in 5% Na_2SO_4. They were then dehydrated in butanol, embedded in paraffin and serially cut on a Reichert microtome (10 μm thick). Serial sections are taken of the skull (exoccipital), the vertebrae and the rocker bone in order to compare the rocker bone with cartilage and bone. Various types of staining methods were applied to the sections (Gabe 1968): alcian blue (pH 3.0)/PAS (periodic acid-Schiff) for the demonstration of glycosaminoglycans (acid mucopolysaccharides) and for proteoglycans respectively, Unna-Tanzer's method for elastic and collagen fibrils, Mallory's trichrome for collagen, toluidine blue for acid mucopolysaccharides and Gallego's method for proteoglycans. Histological sections were observed with an Olympus microscope (Leica DM 100) coupled to a digital camera (Canon Power Shot S50).

Transmission electron microscopy

After glutaraldehyde fixation, rocker bones were demineralised in 0.2 M EDTA (pH 8.0) for 19 days. Samples were dehydrated in an ethanol-propylene oxide series and were then embedded in epoxy resin (SPI-PON 812). The ultrastructure of the rocker bone was examined on ultrathin sections (60–80 nm) stained with uranyl acetate and lead citrate and viewed by a JEOL JEM 100SX transmission electron microscope under an 80-kV accelerating voltage.

Scanning electron microscopy

Ethanol-fixed rocker bones were divided into two groups. The first contained two intact rocker bones for the observation of the external surface. In the second group, five rocker bones were fractured and etched at various times (0, 0.5, 1, 15, 30 and 60 min) in 0.1 N and 1 N HCl. All these pieces were dehydrated through an ethanol series, critical-point dried and platinum sputter-coated (20 nm) in a Balzers SCD-030 sputter-unit. Photographs were taken by using a scanning electron microscope JEOL JSM—840A under a 20-kV accelerating voltage.

Back-scattered electron imaging under SEM

In order to visualise the mineral phase inside the rocker bone by using backscattered electron microscopy (BSE), three rocker bones were dehydrated in 100% ethanol and infiltrated overnight in Epoxy resin. Polymerisation occurred for 3 days at 30°C within an Epofix (Struers) resin. The block faces were trimmed with sagittal, frontal and transversal orientations to a width of several hundred μm in the rocker bone. They were filled with non-aqueous sand paper of decreasing grit sizes (150, 600 grit) and were polished by using a micron diamond suspension (1PS-1MIC ESCIL). The blocks were then rinsed with methanol and were carbon-coated (Balzers MED 010).

Solid-state characterisation

A chemical and structural analysis of the rocker bone was carried out by combining information from several techniques. These experiments were also carried out on two mandibles (from which the teeth and Meckel's cartilage were removed) in order to highlight the differences and similarities between these two mineralised pieces.

Three apatitic phosphates were used for comparison: $Ca_{10}(PO_4)_6(OH)_2$, $Ca_9HPO_4(PO_4)_5OH$, $Ca_8H_2(PO_4)_65H_2O$. Analytical grade $Ca_5(PO_4)_3OH$ was purchased from Riedel-de Haën. Pure $Ca_9(HPO_4)(PO_4)_5(OH)$ was synthesised following the preparation method described by Mortier et al. (1989). $Ca_8(HPO_4)_2(PO_4)_4.5H_2O$ was isolated by applying the precipitation technique described by Legeros (1985).

X-ray diffractograms were collected on a D-5000 powder diffractometer with Ni-filtered copper Kα radiation. Rocker bone and dentary bone samples were prepared either by fine grinding in a mortar or by polishing a cross-

section of a bulk piece. Infrared data were obtained with a Perkin Elmer FTIR spectrometer in the range 400 to 4000 cm^{-1}. Samples of 2 mg of the sample were dispersed in 800 mg oven-dried KBr and pressed into pellets before analysis. Pure KBr was used as a reference. Elemental analysis was carried out by SEM (Philips ESEMFEG XL30) working at 20 kV. The samples were homogenised by grinding and were then placed on carbon tape without any coating. EDX spectra were collected with an EDAX energy dispersive X-ray spectrometer. Pure stoichiometric apatite (Ca/P ratio 1.67, analytical grade $Ca_5(PO_4)_3OH$, purchased from Riedel-de Haën) was used as a standard in order to validate the quantitative analysis. Thermogravimetric curves (TGA) and differential scanning calorimetry (DSC) data were obtained by using a Netsch TG 209 thermobalance, under a 50 ml/min air flux with a 10°C/min heating ramp from room temperature to 1,000°C.

Results

Anatomy

The rocker bone (Fig. 2) is kidney-shaped and situated in front of the swimbladder, below the 2nd, 3rd and 4th vertebrae. This bone appears dense and opaque in X-rays, as indeed do the skeleton and the otoliths (Fig. 2a). The anterior part of the rocker bone is large and bent, whereas the posterior part is narrower and is the site of the insertion of sonic muscles (see Parmentier et al. 2006). The swimbladder (Fig. 2b) is a closed oblong tube situated dorsally in the abdominal cavity and lies firmly applied against the vertebral bodies by means of connective fibres.

Histology

Sagittal and transversal sections of the anterior part of the swimbladder show the presence of several tissue layers (Fig. 3). From the inner to the outer part, the swimbladder includes (1) an inner epithelial tissue (mucosa), (2) a thick layer of elastic fibres (submucosa) and (3) an outer epithelial tissue (serosa). The submucosa appears to be intimately linked to the rocker bone. Indeed, medially, this layer thickens and penetrates the rocker bone (Fig. 3).

The rocker bone itself can be structurally divided into three regions: the peripheral region, the cortical region and the medullar region (Fig. 3).

Peripheral region

The peripheral region consists of an external capsule surrounded by the serosa and is composed of dense tissue in which fibroblasts are well developed (Fig. 4). The

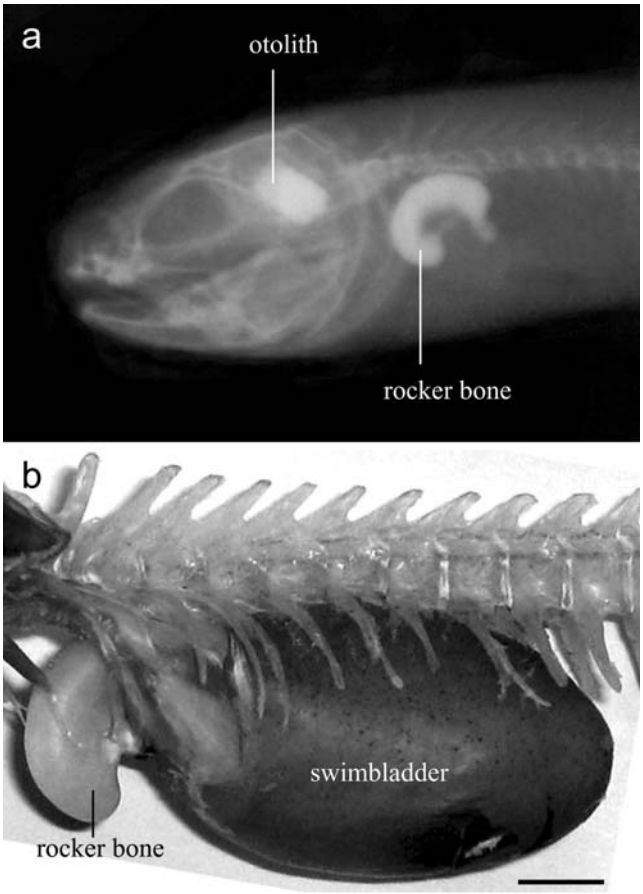

Fig. 2 Left lateral views of the location of the rocker bone of *Ophidion barbatum* revealed (**a**) by X-ray radiography and (**b**) in a dissected specimen. *Bar* 5 mm

innermost fibroblasts exhibit large vacuoles with a flocculent content, sometimes arranged in layers. These vacuoles open regularly at the lower side of the cells, suggesting that exocytosis of their content occurs towards the cortical region of the rocker bone. These secretory vacuoles may correspond to new spherules that are added to those constituting the rocker bone cortex (see below).

Cortical region

The cortical region occupies the greater part of the rocker bone and is highly vascularised (Fig. 3). Staining of the rocker bone with alcian blue/PAS and with the Gallego method highlights the presence of proteoglycans. The metachromasy, when stained with toluidine blue at pH 4.0, indicates that these proteoglycans consist, at least partly, of acid mucopolysaccharides. The cortical region presents a fibrous meshwork with rare isolated cells and blood vessels.

(1) By light microscopy, the fibrous meshwork seemed to delimit small round areas enclosing clear spaces in which the tissues have been demineralised. Observations by SEM revealed that these clear areas were

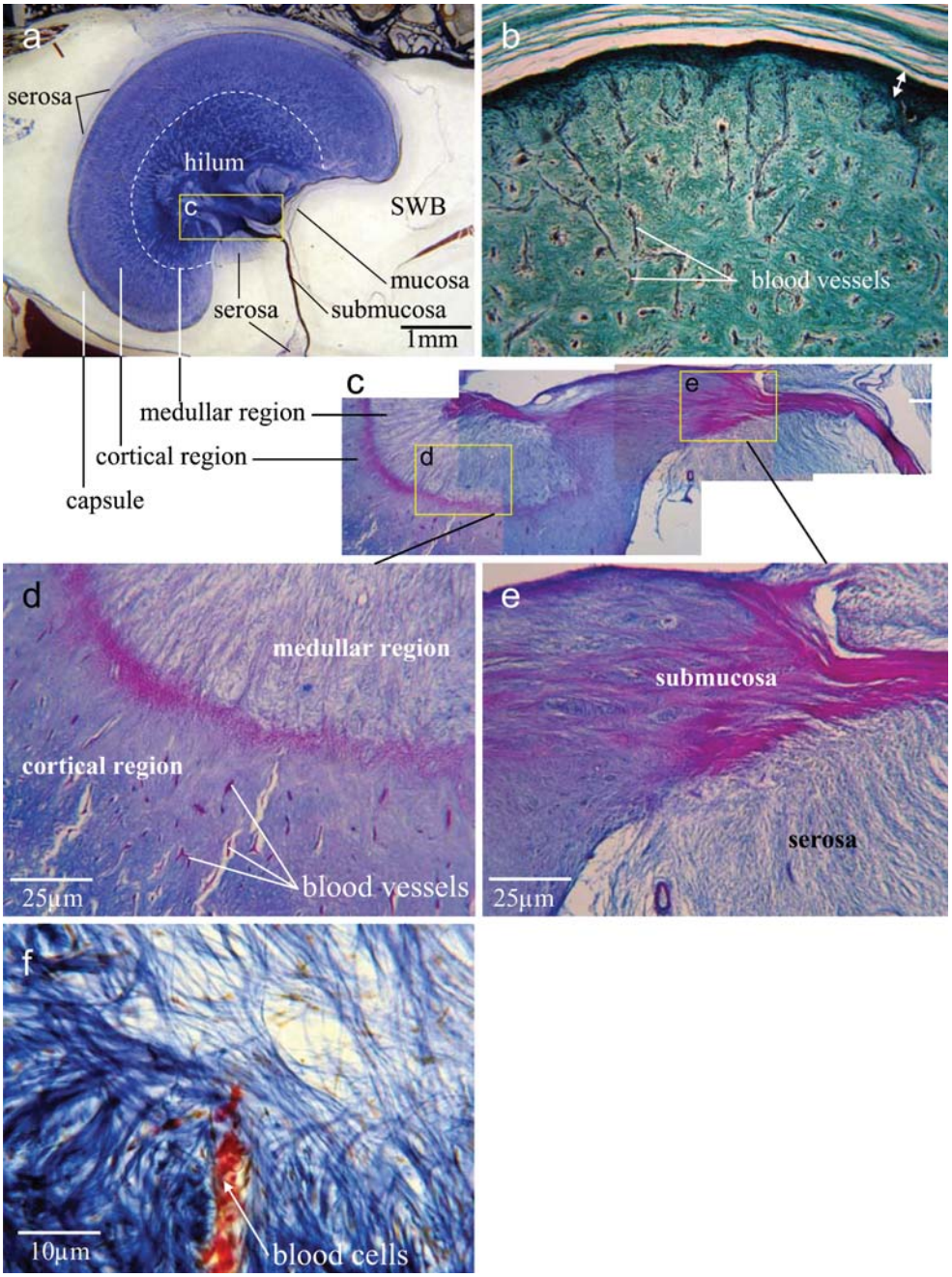

Fig. 3 **a** Left longitudinal section of the rocker bone in *Ophidion barbatum* (*SWB* swimbladder). **b** Dorsal part of the rocker bone showing the capsule (*double arrow*) and the cortical region with blood vessels. **c**, **e** Two successive magnifications of the hilum in **a** showing the continuity of the submucosa in the rocker bone. **d** Separation of the medullar and cortical regions in the rocker bone. **f** Higher magnification of the medullar region. **a**, **f** Mallory staining. **b** Trichrome. **c**–**e** periodic-acid-Schiff.

occupied by mineral spherules of different sizes, with a diameter varying from 1 to 10 µm (Fig. 5). In SEM images of fractured samples, the spherulitic aspect was only visible around blood vessels where fibres were also obvious. The BSE images of polished slices (Fig. 6) showed that these spherules were deeply mineralised (in white), whereas the organic matter and the resin were dark. The size of the spherules was clearly shown to increase from the periphery of the cortex towards the deep cortical region, suggesting that the primordial spherule lay below the capsule and was progressively mineralised. In the deep cortex, the spherules appeared as bright mineral centres surrounded by a less mineralised outer layer. They coalesced with each other (Fig. 5f) to form a compact mineral mass, so that they could not be individually distinguished in fractured samples, except around blood vessels. By TEM, after EDTA demineralisation, each spherule was also found to present a central core surrounded by successive concentric layers of fibrils and granular material; the central core consisted of a central electron-dense granule surrounded by an

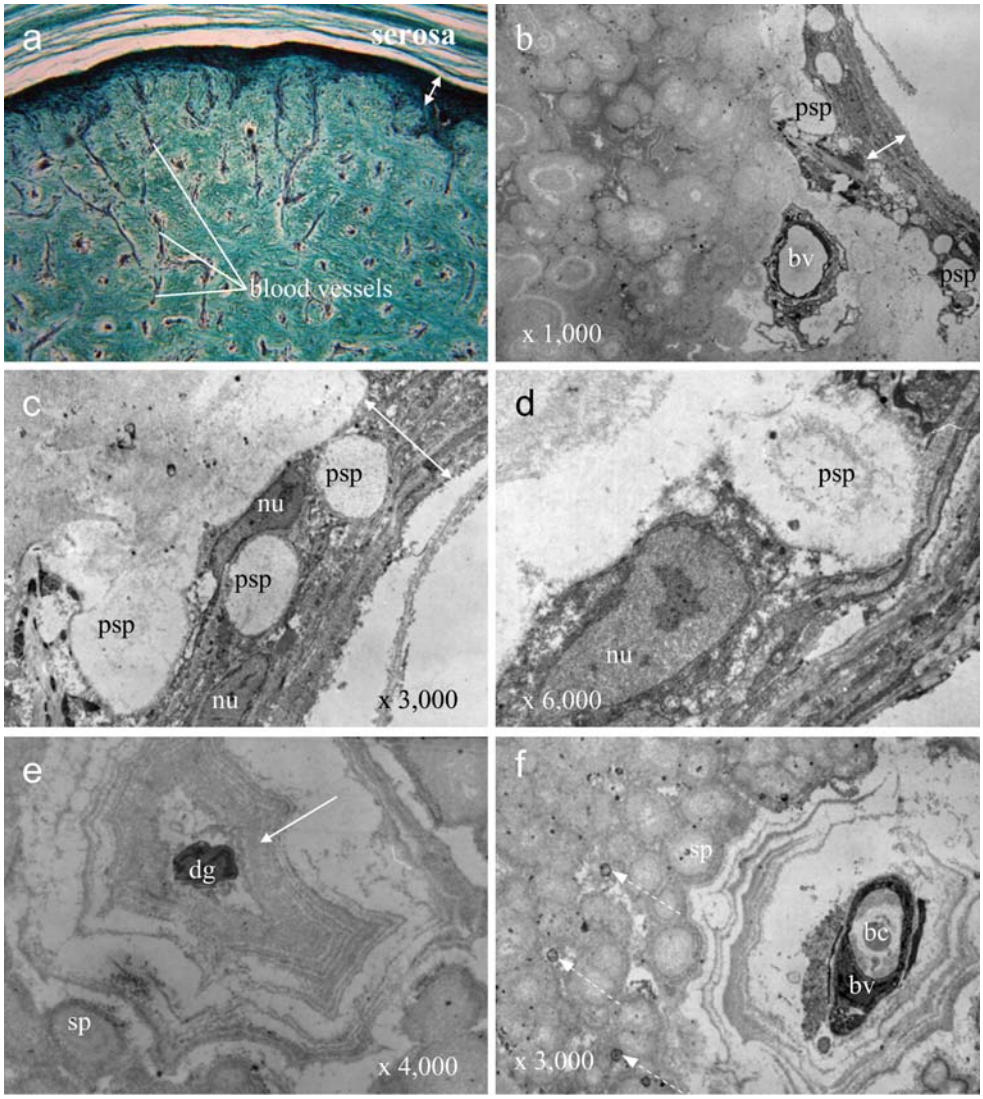

Fig. 4 Rocker bone in *O. barabatum*. **a** Histological section of the capsule (*double arrow*) and the cortical region with blood vessels (same as in Fig. 3b, presented here for ease of comparison with **b–f**). **b–f** Electron micrographs of the capsule (*double arrows*) and cortical region. The primordial spherules (*psp*) are secreted by the capsule (*nu* nucleus of the fibroblast) and seem to migrate towards the cortical region. **e**, **f** Degraded cells (*dg* in **e**) and blood vessels (*bv* blood vessel, *bc* blood cell, *dotted arrows* degraded cells in **f**) are completely surrounded by their own layers of fibrils (*single arrow* in **e**) and by (coalescent) spherules (*sp*)

electron-lucent area. The central core was also discernible under light microscopy in the centre of different clear spaces and by SEM imaging after the mineral had been dissolved with HCl (Fig. 7). The surrounding layers represented the distribution of intraspherulitic organic matter and fibrils (Fig. 5). The orientation of the fibrils was globally radial, as also suggested by the SEM images of fibres radiating from the spherule centre in HCl-treated samples. These fibrils did not present the typical periodicity of type I or type II collagen. The electron-dense granular material associated with the fibrils was probably constituted by proteoglycans (Fig. 5h). In many places, and especially close to the blood vessels, an additional layered material was found either in the spaces between the spherules or embedding several neighbouring spherules. The presence of this material suggested that the spherules were united by a mineralised cement. This was confirmed by the finding that fractures in the compact cortex of the rocker bone presented small vitreous surfaces without spaces between the spherules (Fig. 5b,c).

(2) Isolated cells were mainly found underneath the fibroblast layer (Fig. 4e), close to the capsule. Deeper in the cortex, they appeared to become smaller with a pyknotic nucleus and then to degenerate into small fragments of necrosed cells between the spherules (Fig. 4f). The orientation and disposition of the fibrillar and granular material that surrounded the degrading cells indicated that these materials were secreted by the cells themselves (Fig. 4e).

(3) Blood vessels were frequently found in the cortical region of the rocker bone. By SEM, they were seen to run in unmineralised canals between the

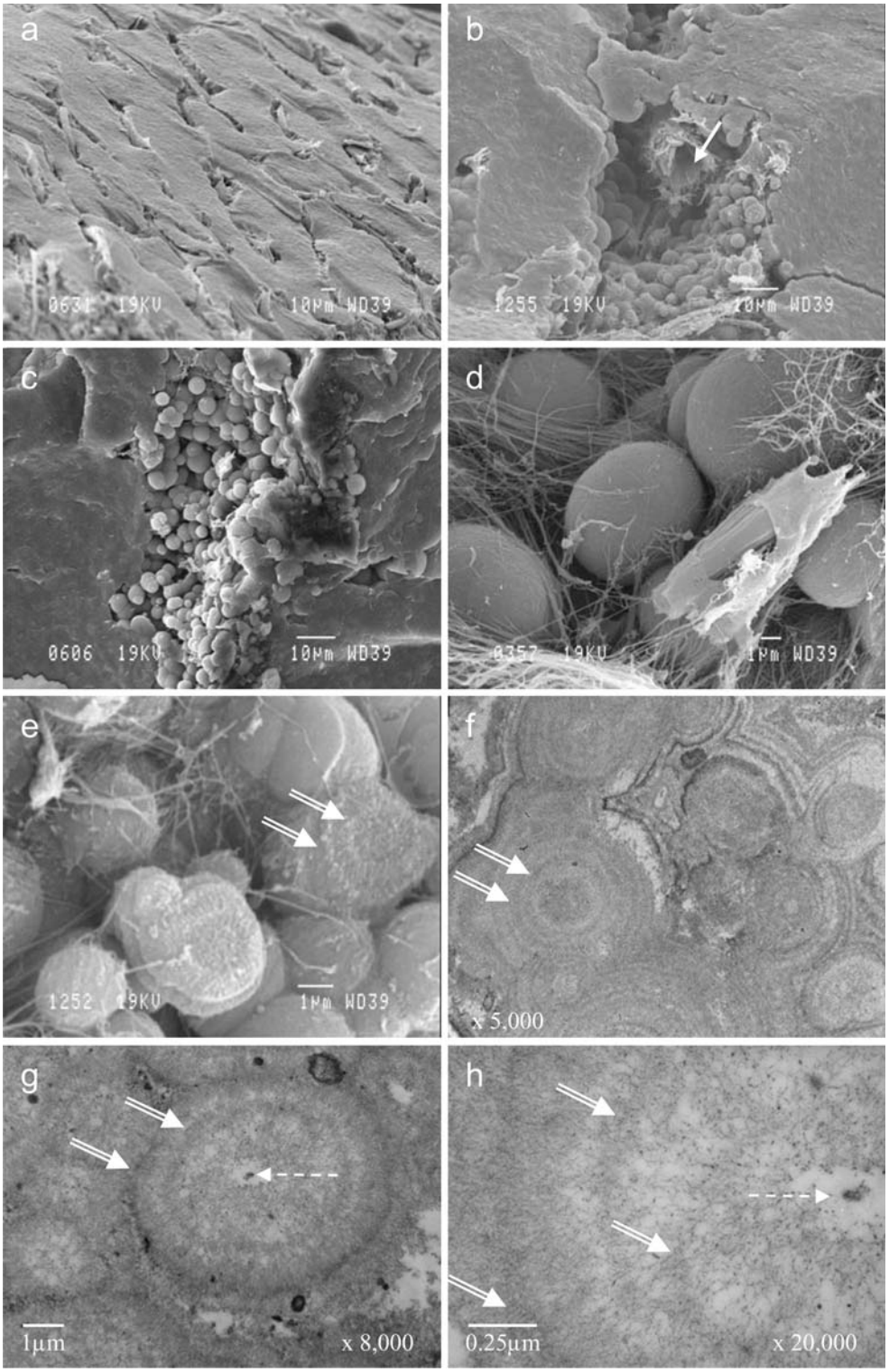

Fig. 5 Details of the rocker bone in *O. barbatum*. **a–e** SEM. **a** External surface of the rocker bone. **b–e** The rocker bone was broken apart in order to reveal the internal components of the cortical region. **b** Spherules adjacent to a blood vessel (*white arrow*). **c**, **d** Spherules surrounded by fibrils. **e** Degraded spherules with a view of the concentric layers (*double white arrows*). **f–h** TEM. Concentric layers in (adjacent) spherules (*dotted arrows* central core of electron-dense material)

spherules. TEM revealed that the blood vessel endothelia were often surrounded by organic matter (Fig. 4f). The canal walls exhibited the protuberant surface of the spherules but the spherules did not seem to crush the vessels. The blood vessels formed a branching network through the whole cortex, reaching up to the capsule but never passing through it (Fig. 5b).

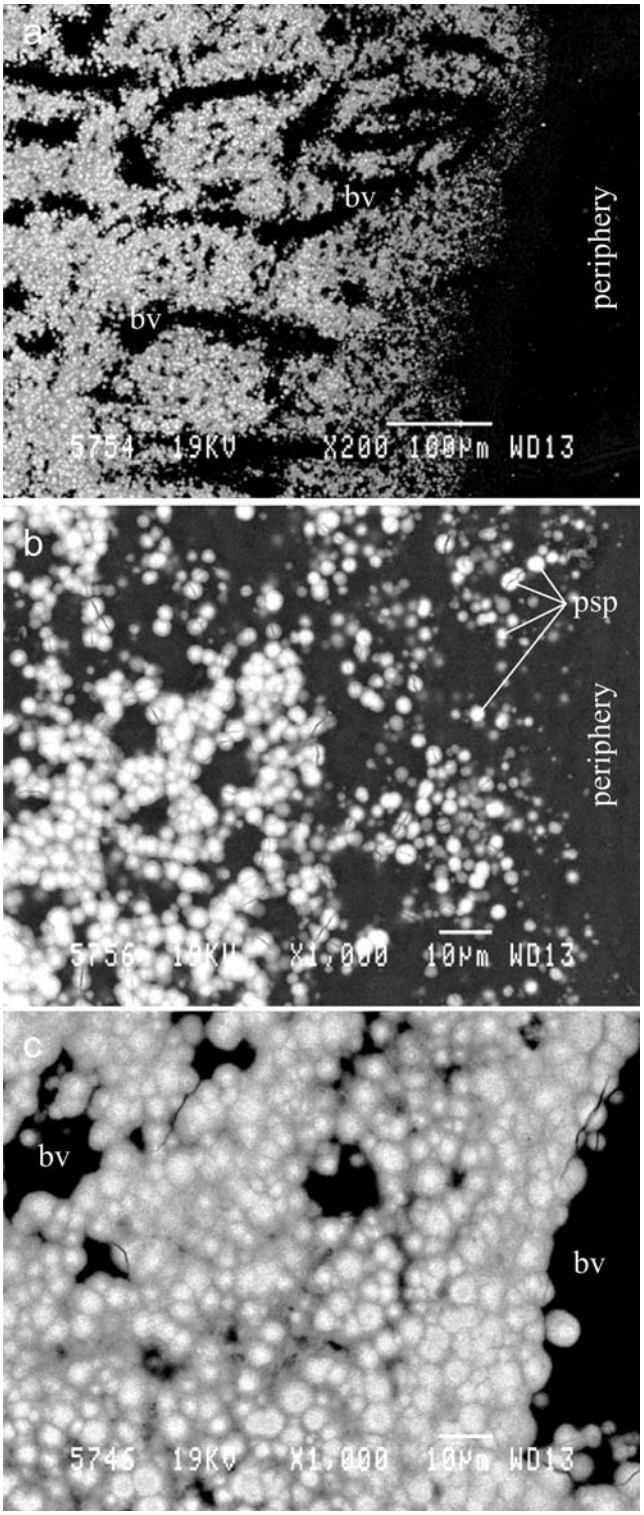

Fig. 6 Back-scattered electron imaging (under SEM) of the mineral part of the spherules (*white*) in the rocker bone of *O. barbatum*. The variability in the whiteness is attributable to the rate of mineralisation and to the size of the spherules (*black areas* amorphous organic structure, *bv* blood vessel, *psp* primordial spherule)

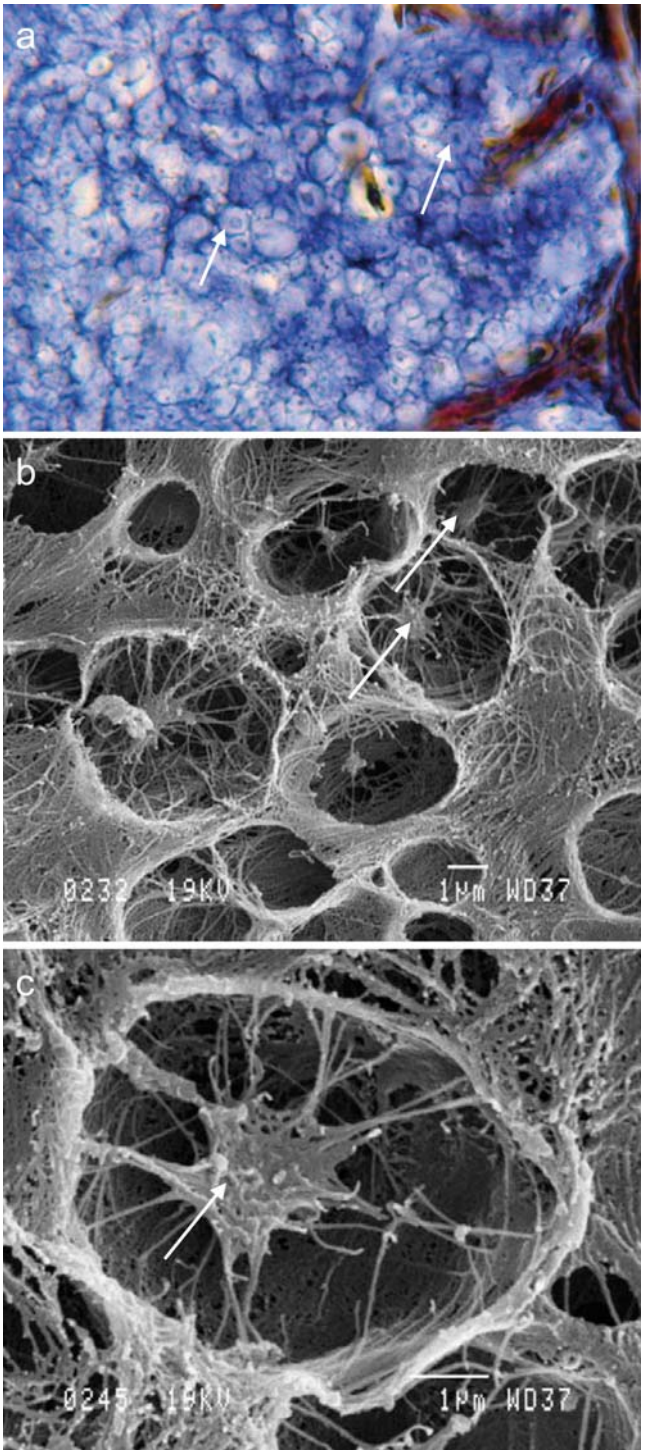

Fig. 7 Histological section (**a**) and SEM views (**b**, **c**) of the cortical region of the rocker bone in *O. barbatum* (*white arrows* remaining fibres in the centre of the spherule after demineralisation. **b**, **c** Rocker bone exposed to 1 N HCl for 60 min

Medullar region

The medullar region (or hilum) occupies the centre of the rocker bone (Fig. 3). It is mainly fibrous. This region is also less mineralised and is not clearly visible under X-rays

(Fig. 2a). The blood vessels penetrate into the rocker bone at the level of the hilum. They first reach the medullary region before dividing into smaller vessels that form a dense network in the cortical region.

Mandible and vertabrae

The mandible bone and vertebrae were used for histological comparisons. Generally speaking, the alcian blue/PAS stain stained the rocker bone and the (hyaline) cartilage of the exoccipital and neural spine blue and the mandible bone red. By SEM, the organisation of the mandible bone was found to be one of classical bone in fish (Fig. 8): it was acellular and consisted of a lattice of plates and struts. Collagen fibrils lay parallel to each other to form lamellae. These lamellae were ordered into thin sheets, which were subsequently interwoven by perpendicular fibres. The dentary and vertebral bones lacked spherules and did not possess a well-developed vascularised network.

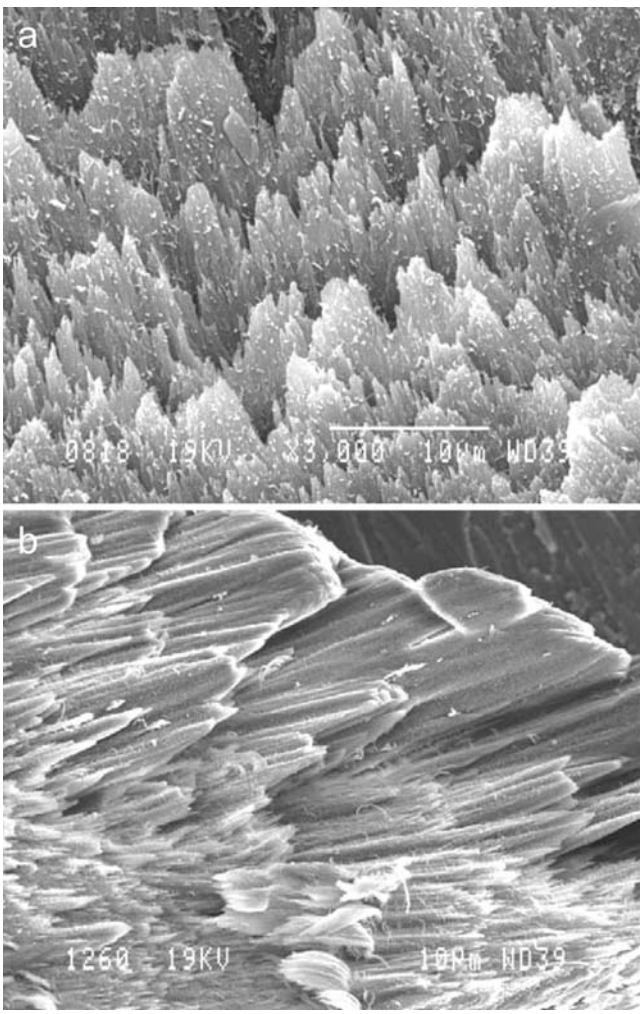

Fig. 8 SEM. Inside view of the bone of a broken mandible of *O. barbatum*

Chemical analysis of the rocker bone

The most frequently encountered mineral constituents in vertebrate bones belong to the so-called "bioapatite" group. These minerals are calcium phosphates with a crystal structure derived from the hydroxyapatite $Ca_{10}(PO_4)_6(OH)_2$. Numerous ion substitutions occur naturally and give rise to a large number of stoichiometries, with possible solid solution between them. Three well-defined compositions will be used as a basis for discussion: $Ca_{10}(PO_4)_6(OH)_2$, $Ca_9HPO_4(PO_4)_5OH$, $Ca_8H_2(PO_4)_65H_2O$ (hereafter named Ca_{10}, Ca_9 and Ca_8, respectively). The Ca_{10} mineral is the main component of bone (Stevens and Lowe 1997), whereas Ca_8 is identified as a precursor of mineralisation in teeth and bone formation (Elliott 1994). Ca_9 is an intermediate Ca-deficient mineral, whose structure is well-established (for a complete description of the structure and chemistry of calcium orthophosphates, see Elliott 1994).

X-ray diffraction is the most common method used to identify a crystal structure. However, all minerals derived from apatite produce similar diffractograms and additional forms of characterisation have to be used to discriminate between them. In this study, diffractograms of the rocker bone were compared with the Ca_{10}, Ca_9 and Ca_8 reference data from the X-ray diffraction database (JCPDF). Only Ca_8 could be excluded because of the lack of two peaks around 10°2θ.

Infrared spectra (Fig. 9) confirmed the lack of correspondence between the mineral present in the rocker bone and the Ca_8 structure, as could be particularly well seen in the phosphate absorption region around 1,000 cm^{-1}. Here, Ca_8 was found to exhibit a typical fine vibrational pattern composed of more than three sharp peaks. By contrast, the bone and rocker bone samples showed a large and smooth absorption band. Moreover, some differences could be noticed from the Ca_{10} mineral, especially in the hydroxyl absorption region, where unbridged ^{-}OH groups were seen to give rise to a sharp and intense peak at 3,600 cm^{-1} for the Ca_{10}. Indeed, in the crystal structure of $Ca_{10}(PO_4)_6(OH)_2$, the hydroxyl groups are located within the layers and are arranged in such a sequence that no hydrogen bridging is possible between them (Posner et al. 1958; Hughes et al. 1989). Instead, the rocker bone shows a large absorption peak typical for hydrogen-bonded hydroxyl groups. Another characteristic peak of Ca_{10} was found to be missing at 640 cm^{-1}.

On the other hand, an excellent correspondence was established between the rocker bone apatite mineral and the Ca_9 spectra, even in the fingerprint region. Finally, the rocker bone and the reference bone (dentary) were compared with each other and were found to have similar infrared spectra. Infrared analysis thus suggested a Ca_9-like crystal structure for both the rocker bone and the dentary bone.

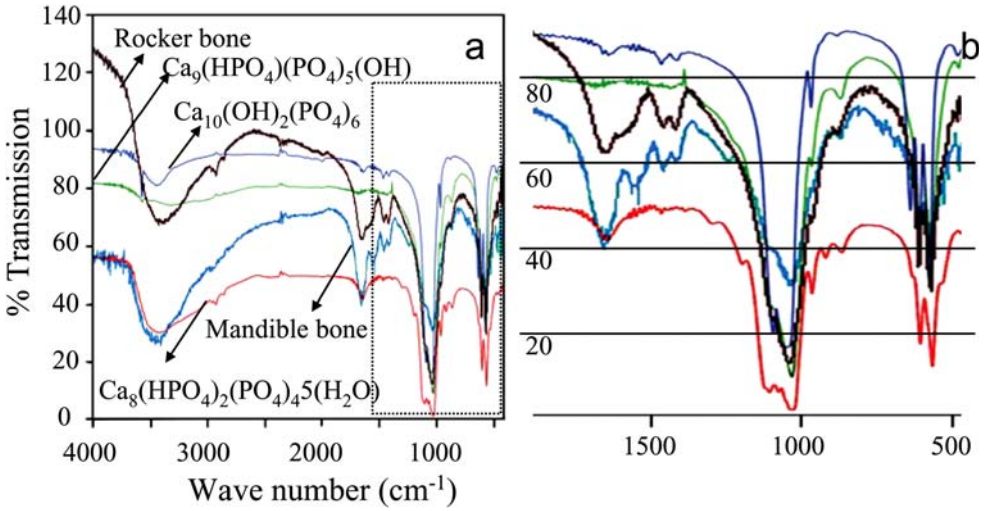

Fig. 9 **a** Infrared spectrum of the rocker bone (*black*) and the mandible bone (*vivid blue*) of *O. barbatum* compared with hydroxyapatite Ca_{10} (*dull blue*), Ca_9 (*green*) and Ca_8 (*red*). **b** Enlarged part of *boxed area* in **a**

Elemental analysis provided additional information regarding the chemical composition of the rocker bone. The Ca/P ratios calculated for Ca_{10}, Ca_9 and Ca_8 were 1.67, 1.50 and 1.33, respectively. Both the rocker bone and mandible bone were found to be characterised by a Ca/P ratio of 1.46 and 1.41, respectively. These values are close to each other but somewhat lower than the expected value for a Ca_{10} or Ca_9 stoichiometry. This can be explained by a significant concentration of substituted cations, viz. Na^+ and Mg^{++}, detected by the EDX spectrometer. These cations partially replace the Ca^{++} ions in the crystal structure, especially in apatites of biological origin.

Finally, thermogravimetric experiments were performed in order to confirm or deny the presence of Ca_{10}. Indeed, this mineral is known to be thermally stable up to 1,000°C (Locardi et al. 1993; Zhou et al. 1993), whereas Ca_9 decomposes into $Ca_3(PO_4)_2$. Intermediate compositions gave a mixture of Ca_{10} and $Ca_3(PO_4)_2$ after calcination at 1,000°C. TGA curves showed that the rocker bone constituent was not stable up to 1,000°C but underwent a significant multi-step mass loss, associated with an exothermic peak at between 100°C and 500°C in the DSC curve. Of course, this complex decomposition process included not only the production of water at low temperature and combustion of organic species, but also the degradation of the inorganic phase into $Ca_3(PO_4)_2$ and the remaining Ca_{10}, as confirmed by X-ray diffraction of the final residue. The dry inorganic residue at 1,000°C constituted 78% of the weight of the initial rocker bone and 63% of the weight of the initial mandible bone.

As a conclusion to this chemical and structural analysis, no difference could be evidenced between the mineral structure of mandible bone and rocker bone. Several experiments confirmed that the rocker bone was composed of a bioapatite of stoichiometry between Ca_{10} and Ca_9, with a crystal structure close to Ca_9 and a significant substitution of Ca^{++} by Na^+ and Mg^{++} ions.

Discussion

In teleosts, the swimbladder can be defined as a hollow organ that is a diverticulum of the digestive tract; this implies that it is made of the same types of tissue. Three types of tissues can be found in the swimbladder of *O. barbatum*: (1) an inner epithelial layer (mucosa), (2) a thick layer of (at least) elastic fibres (submucosa), and (3) a second epithelial layer, the serosa (Parmentier et al. 2006). In *O. barbatum*, the serosa completely surrounds the rocker bone, whereas the submucosa is intimately connected to it (Parmentier et al. 2006). The submucosa thickens medially and penetrates and ramifies into the rocker bone organic matrix (Fig. 3e). This configuration suggests that the rocker bone results from modifications of the serosa and the submucosa. The carapids (sister family of the Ophidiidae) of the *Onuxodon* genus also present a so-called "rocker bone" in front of the swimbladder (Parmentier and Diogo 2006). Comparisons of the swimbladder in different Carapidae genera has led to the hypothesis that this "rocker bone" is homologous with the anterior part of the swimbladder and is a response to the mechanical stress of the traction transmitted by the various ligaments and muscles inserted upon it (Parmentier et al. 2002).

The type of connective tissue varies according to the abundance and type of cell, to the proportion of cells in the matrix and to the properties of the matrix itself, including the number and type of fibres and the nature of the ground substance. The present histological and ultrastructural studies, together with the various analyses that we have carried out, have enabled us to ascertain that the rocker

bone does not correspond to a form of cartilage, as previously noted (Rose 1961; Matallanas 1980; Howes 1992). In fishes, eight types of cartilage have been identified and categorised into two groups: cell-rich cartilage and matrix-rich cartilage (Benjamin 1990). In cell-rich cartilage, >50% of the tissue volume comprises of cells rather than extracellular matrix. This is not the case in the rocker bone. Moreover, spherical cell morphology seems to be critical for the production of cartilage-specific matrix molecules within vertebrates (see Benjamin et al. 1994 for a review). The rocker bone cells present neither a rounded morphology (as is usually the case in hyaline), nor elastic fibres or fibro-cartilage (Beresford 1981; Cole and Hall 2004a, 2004b). Except for those cells in blood vessel endothelium and in the capsule, most of the cells within the rocker bone are degraded or fragmented, and the rocker bone matter appears to be acellular. In addition, the rocker bone does not present type II collagen and is highly vascularised, which is not the case in fish cartilage (Meunier and François 1992).

Beresford (1981, 1993) has categorised chondroid bone into two general types: CB I and CB II. CB II consists of chondrocyte-like cells in a bony matrix (Huysseune 1986; Huysseune and Verraes 1986; Meunier and Huysseune 1992; Beresford 1993). The rocker bone does not present chondrocyte-like cells but the matrix composition (fibrils and proteoglycans) is close to the cartilage matrix. Moreover, CB II is usually described as "articular tissue" in close association with bone (Huysseune and Sire 1990), which is not the case here. CB I is usually described as a short-lived intermediate form of tissue. CB I generally accompanies new bone and cartilage, thus linking these two tissues physically. CB I is also found uniting superficial bone or is involved in cranial joints (Beresford 1981, 1993). These criteria are not found in the rocker bone.

Superficially, some analogies between the rocker bone and true fish bones can be drawn from their general organisation and composition. Bones present a layer of dense connective tissue (periosteum) surrounding a compact zone and a more inner spongious area (Gartner and Hiatt 1997; Toppets et al. 2004). Similarly, the rocker bone presents three layers: the external capsule, the intermediate cortical region and the inner medullar zone. However, different characteristics distinguish bone from the rocker bone. Bone is typically made up of three components (Meunier and François 1992; Meunier and Huysseune 1992): (1) bone cells, (2) collagen fibrils and proteoglycans and (3) hydroxyapatite crystals. The rocker bone possesses only hydroxyapatite and proteoglycans. Moreover, the cells inside the rocker bone are not osteocytes; they do not show the characteristic canaliculi, they are often completely sequestered by the extracellular matrix and most of them appear to be necrosed.

In bones, collagen fibrils (type I) constitute the main component of the osteoid (Zhengwen et al. 2005); they form a woven network, on which the mineral salts precipitate (Stevens and Lowe 1997; Weiner and Wagner 1998). Hydroxyapatite crystals consist of platelets (80×30×8 nm) closely associated with fibrils having a periodicity of 67 nm corresponding to the gap zones in the type I collagen fibrils. Instead of collagen fibrils, the rocker bone matter contains thin fibrils, which do not correspond to any of the classical collagen fibrils because of their small diameter and the absence of banding. Histochemical data suggest instead that proteoglycans are contained within rocker bone matter. In addition, the spherulitic organisation of the mineral within the rocker bone contrasts with the disposition of the hydroxyapatite crystals in bone. Each spherule is probably composed of small acicular mineral units radially distributed from the central nucleus in parallel to the fibrils. This microcrystalline mineral structure is supported by TEM observations and by the smooth (vitreous) fracture surfaces observed by SEM. The rocker bone also contains a meshwork of thicker fibrils, which could be collagen, but these are external to the mineral spherules. The fibrils may be trapped in the cement with the isolated cell fragments; these have not been discerned in the ultra-thin sections examined in the present study.

Three processes occur in primary bone formation: intramembranous, endochondral and periostic ossification. In the first two ossification processes, pre-existing connective tissue (mesenchymal and cartilaginous models, respectively) is replaced by bone but this is not the case in the rocker bone. The formation of the rocker bone resembles periostic ossification. Indeed, the rocker bone seems to be continuously elaborated by the innermost fibroblast layer of the capsule. These mineral-secreting fibroblasts might be analogous to bone osteoblasts. However, in contrast to osteoblasts, they do not secrete collagen fibres towards the rocker bone, whereas banded collagen fibres are easily recognisable in the capsule. Spherule formation appears to be initiated intracellularly inside vacuoles of the fibroblasts; these vacuoles are exocytosed as small units with a central core that is probably mineralised. TEM and BSE-SEM images suggest that the spherules continue their growth extracellularly, until they meet the neighbouring spherules. The spaces between them are finally filled by cement. The cement shows the same layered appearance and mineral composition (X-ray microanalyses) as the spherules themselves. Its location suggests that the cement is secreted by the isolated cells below the capsule and around the blood vessels before the cells become completely trapped in the structure and undergo necrotic fragmentation. This elaboration process of the rocker bone is markedly different from the deposition of bone by osteoblasts, which secrete successively and independently the bone matrix (collagen

and proteoglycans) and the mineral ions in small vesicles by exocytosis (Toppets et al. 2004).

Unlike for bone, no evidence is apparent of a secondary reconstruction process in the rocker bone and no traces occur of osteoclasts or analogous cells. Only the medullar region is more fibrous, containing more blood vessels and fewer spherules, probably because of secondary mobilisation of the mineral around the blood vessels that develop with the growth of the rocker bone. The blood vessels probably transport the materials necessary for the elaboration of the rocker bone through the structure and towards the capsule. They elongate and ramify towards the capsule with the growth of the rocker bone.

Bone minerals are well established as being mainly constituted by calcium hydroxyapatite with a variable composition, generally called "bioapatite" (Dalconi et al. 2003; Wopenka and Pasteris 2005). However, the rocker bone appears to be highly mineralised: the mineral mass corresponds to 78% of the total mass. Generally speaking, this value is between only 60% and 70% in bone (Toppets et al. 2004; Zhengwen et al. 2005; the present study). In the present study, the different approaches show that the mineral phase is the same for both dentary bone and the rocker bone. However, the exact determination of the composition of a particular bioapatite is difficult because of its weak crystallisation and the presence of organic compounds disturbing its characterisation (Skinner 2000). Moreover, apatite is a flexible mineral, which means that it is accommodating to chemical substitutions. Such ionic substitutions slightly change the structure of a mineral and often have critical effects on its mineral properties (Dalconi et al. 2003; Penel et al. 2005). Among the substituting ions that are known and/or that have been reported in bone are F^-, Cl^-, Na^+, K^+, Fe^{2+}, Zn^{2+}, Sr^{2+}, Mg^{2+}, citrate and carbonate (Wopenka and Pasteris 2005). As expected, Na^+ and Mg^{2+} have been detected here in the rocker bone. According to our results, the mineral of the rocker bone is characterised by a stoichiometry comprised of $Ca_{10}(PO_4)_6(OH)_2$ and $Ca_9HPO_4(PO_4)_5OH$ hydroxyapatites. These minerals might form an intermediate solid solution, partly substituted by Na^+ and Mg^{2+} ions. On the other hand, the rocker bone could be biphasic and composed of Ca_{10} and Ca_9, the latter being more important. The hypothesis of a biphasic structure is reinforced by the production of a biphasic calcium phosphate, consisting of hydroxyapatite Ca_{10} and tricalcium phosphate $Ca_3(PO_4)_2$ (Victoria and Gnanam 2002).

In conclusion, the rocker bone is a hard vascularised skeletal structure situated at the front of the swimbladder and is derived from the serosa and the submucosa. This kidney-shaped structure is made up of three different regions: the capsule, the cortex and the medullar regions. It represents a new kind of mineralised tissue with (1) a ground substance containing proteoglycans and fibres and (2) a matrix containing small mineral spherules. The latter are composed of a bioapatite (hydroxyapatite) and concentric layers of non-oriented fibrils and granular material around a central core. Neither the ground substance nor the spherules present recognisable type I or II collagen fibres. The rocker bone grows via the apposition of new spherules at its periphery. The formation of the spherules starts intracellularly inside vacuoles of fibroblasts in the capsule and then the growth is extracellular. Cells are also found in the ground substance; their involvement in rocker bone formation through the elaboration of a cement between the spherules leads to their isolation and their necrosis. The presence of spherules of different sizes, the observation that some of these are coalescent and the peculiarity of the rocker bone in presenting a smooth surface when fractured leads us to propose calling this kind of biomineral "frigolite", the Belgian name for styrofoam.

Acknowledgments The authors thank N. Decloux for her technical assistance with the histology and electron microscopy.

References

Benjamin M (1990) The cranial cartilages of teleosts and their classification. J Anat 169:153–172

Benjamin M, Archer CW, Ralphs JR (1994) Cytoskeleton of cartilage cells. Microsc Res Tech 28:372–377

Beresford WA (1981) Chondroid bone, secondary cartilage and metaplasia. Urban and Schwarzenberg, Baltimore

Beresford WA (1993) Cranial skeletal tissue: diversity and evolutionary trends. In: Hanken J, Hall BK (eds) The skull vol 2. University of Chicago Press, Chicago, pp 69–130

Cole AG, Hall BK (2004a) Cartilage is a metazoan tissue; integrating data from nonvertebrate sources. Acta Zool 85:69–80

Cole AG, Hall BK (2004b) The nature and significance of invertebrate cartilages revisited: distribution and histology of cartilage and cartilage-like tissues within the Metazoa. Zoology 107:261–274

Dalconi MC, Meneghini C, Nuzzo S, Wenk R, Mobilio S (2003) Structure of bioapatite in human foetal bones: an X-ray diffraction study. Nucl Inst Met B 200:406–410

Elliott JC (1994) Structure and chemistry of the apatites and other calcium orthophosphates. Studies in inorganic chemistry, vol 18. Elsevier Science, Amsterdam

Gabe M (1968) Techniques histologiques. Masson et Cie, Paris

Gartner LP, Hiatt JL (1997) Atlas en couleur d'histologie. Pradel, Paris

Howes GJ (1992) Notes on the anatomy and classification of Ophidiiform fishes with particular references to the abyssal genus *Acanthonus* Günther, 1878. Bull Br Mus Nat Hist Zool 58:95–131

Hughes JM, Cameron M, Crowley KD (1989) Structural variations in natural F, OH, and Cl apatites. Am Miner 74:870–876

Huysseune A (1986) Late skeletal development at the articulation between upper pharyngeal jaws and neurocranial base in the fish, *Astatotilapia elegans*, with the participation of a chondroid form of bone. Am J Anat 177:119–137

Huysseune A, Sire JY (1990) Ultrastructural observations on chondroid bone in the teleost fish *Hemichromis bimaculatus*. Tissue Cell 22:371–383

Huysseune A, Sire JY (1992) Development of cartilage and bone tissues of the anterior part of the mandible in cichlid fish: a light and TEM study. Anat Rec 233:357–375

Huysseune A, Verraes W (1986) Chondroid bone on the upper pharyngeal jaws and neurocranial base in tha adult fish *Astatotilapia elegans*. Am J Anat 177:527–535

Legeros RZ (1985) Preparation of octacalcium phosphate (OCP): a direct fast method. Calcif Tissue Int 37:194–197

Locardi B, Pazzaglia UE, Gabbi C, Profilo B (1993) Thermal behaviour of hydroxyapatite intended for medical applications. Biomaterials 14:437–441

Matallanas J (1980) Etude de l'alimentation d'*Ophidion barbatum* (Pisces, Ophidiidae) dans la mer catalane. Cybium 1980:81–89

Meunier FJ (1989) The acellularization process in osteichthyan bone. In: Splechtna H, Hilgers H (eds) Trends in vertebrate morphology. Fischer, Stuttgart, pp 443–446

Meunier FJ, François Y (1992) Croissance du squelette chez les Téléostéens. I. Squelette, os, tissus squelettiques. Ann Biol 31:169–184

Meunier FJ, Huysseune A (1992) The concept of bone tissue in Osteichthyes. Neth J Zool 42:445–458

Mortier A, Lemaitre J, Rodrique L, Rouxhet PG (1989) Synthesis and thermal behaviour of well-crystallized calcium-deficient phosphate apatite. J Solid State Chem 78:215–219

Moss ML (1961) Studies of the acellular bone of teleost fish. Acta Anat 46:343–462

Moss ML (1963) The biology of acellular teleost bone. Ann N Y Acad Sci 109:227–350

Parmentier E, Diogo R (2006) Evolutionary trends of swimbladder sound mechanisms in some teleost fishes. In: Ladich F, Collin SP, Moller P, Kapoor BG (eds) Fish communication. Science, USA, pp 43–68

Parmentier E, Chardon M, Vandewalle P (2002) Preliminary study on the ecomorphological signification of the sound-producing complex in Carapidae. In: Aerts PD, Août K, Herrel A, Van Damme R (eds) Topics in functional and ecological vertebrate morphology. Shaker, Maastricht, pp 139–151

Parmentier E, Gennotte V, Focant B, Goffinet G, Vandewalle P (2003a) Characterization of the primary sonic muscles in *Carapus acus* (Carapidae): a multidisciplinary approach. Proc R Soc Lond [Biol] 270:2301–2308

Parmentier E, Vandewalle P, Lagardère JP (2003b) Sound-producing mechanisms and recordings in Carapini species (Teleostei, Pisces). J Comp Physiol [A] 189:283–292

Parmentier E, Fontenelle N, Fine ML, Vandewalle P, Henrist C (2006) Functional morphology of the sonic apparatus in *Ophidion barbatum* (Teleostei, Ophidiidae). J Morphol 267:1461–1648

Penel G, Delfosse C, Descamps M, Leroy G (2005) Composition of bone and apatitic biomaterials as revealed by intravital Raman microspectroscopy. Bone 36:893–901

Posner AS, Perloff A, Diorio AF (1958) Refinement of the hydroxyapatite structure. Acta Cryst 11:308–309

Rose JA (1961) Anatomy and sexual dimorphism of the swim bladder and vertebral column in *Ophidion holbrooki* (Pisces: Ophidiidae). Bull Mar Sci Gulf Carib 11:280–307

Skinner HCW (2000) Minerals and human health. In: Vaughan DJ, Wogelius RA (eds) Environmental mineralogy, European union of mineralogy. Eotvos University Press, Budapest, pp 383–412

Stevens A, Lowe J (1997) Histologie humaine. DeBoeck & Larcier, Bruxelles

Toppets V, Pastoret V, De Behr V, Antoine N, Dessy C, Gabriel A (2004) Morphologie, croissance et remaniement du tissu osseux. Ann Med Vet 148:1–13

Victoria EC, Gnanam FD (2002) Synthesis and characterisation of biphasic calcium phosphate. Trends Biomater Artif Organs 16:12–14

Weiner S, Wagner HD (1998) The material bone: structure-mechanical function relations. Annu Rev Mater Sci 28:271–298

Wopenka B, Pasteris JD (2005) A mineralogical perspective on the apatite in bones. Mater Sci Eng 25:131–143

Zhengwen Y, Yinshan J, Li xin Y, Bo W, Fangfei L, Shemmei S, Tianyi H (2005) Preparation and characterization of magnesium doped hydroxyapatite-gelatin nanocomposite. J Mater Chem 15:1807–1811

Zhou J, Zhang X, Chen J, Zeng S, De Groot K (1993) High temperature characteristics of synthetic hydroxyapatite. J Mater Sci Mater Med 4:83–85